

Generalized functional dynamic principal component analysis

Tzung Hsuen Khoo¹, Issa-Mbenard Dabo²,
Dharini Pathmanathan¹, Sophie Dabo-Niang³

¹Institute of Mathematical Sciences, Faculty of Science, Universiti
Malaya, 50603, Kuala Lumpur, Malaysia.

²Institut de mathématiques de Bordeaux, University of Bordeaux,
France.

³CNRS, UMR 8524-Laboratoire Paul Painlevé, INRIA-MODAL,
Université Lille, F-59000, Lille, France.

Contributing authors: 17201135@siswa.um.edu.my;
issa-mbenard.dabo@math.u-bordeaux.fr; [dharini@um.edu.my](mailto:धारिणी@um.edu.my);
sophie.dabo@univ-lille.fr;

Abstract

In this paper, we explore dimension reduction for time series of functional data ($\mathbf{X}_t : t \in \mathbb{Z}$) within both stationary and non-stationary frameworks. We introduce a functional framework of generalized dynamic principal component analysis (GDPCA). The concept of GDPCA aims for better adaptation to possible non-stationary features of the series. We define the functional generalized dynamic principal component (GDPC) as static factor time series in a functional dynamic factor model and obtain the multivariate GDPC from a truncation of the functional dynamic factor model. GDFPCA uses a minimum squared error criterion to evaluate the reconstruction of the original functional time series. The computation of GDPC involves a two-step estimation of the coefficient vector of the loading curves in a basis expansion. We provide a proof of the consistency of the reconstruction of the original functional time series with GDPC converging in mean square to the original functional time series. Monte Carlo simulation studies indicate that the proposed GDFPCA is comparable to dynamic functional principal component analysis (DFPCA) when the data generating process is stationary, and outperforms DFPCA and FPCA when the data generating process is non-stationary. The results of applications to real data reaffirm the findings in simulation studies.

Keywords: Dimensionality reduction, Functional data analysis, Principal component analysis, Dynamic factor models

1 Introduction

The recent advances in computing, coupled with the ability to collect and store high-dimensional data have empowered statisticians to explore models specifically tailored for high-dimensional data. Analyzing high dimensional data in various fields ranging from science to economics had a great impact on statistical approaches employed in modelling, displaying and forecasting high dimensional data. A dimensionality reduction approach with the flexibility of being data dependent allows statistical models to adapt to the characteristics and complexity of the data without imposing rigid assumptions or constraints. A challenge with dimensionality reduction in economics and finance is that numerous time series encountered within these fields exhibit nonstationarity. Therefore, a versatile dimensionality reduction approach from the non-stationary time series perspective that captures relevant information, such as fluctuations and uncertainties, thereby enhancing accuracy in modeling, is essential. This led to the formulation of generalized dynamic principal component analysis (GDPCA) (Peña and Yohai, 2016) which fulfilled the aforementioned criteria and serves as motivation for this work from a functional data perspective.

Functional data analysis (FDA) is proven to be valuable in the context of high-dimensional datasets where discrete observations are presented as functions, forming functional data where an entire measured function is treated as a singular observation. Subsequently, statistical principles from multivariate analysis are employed to model and analyze collections of functional data. Ramsay and Silverman (2005) provided an in-depth and authoritative exploration of the fundamental principles and practical applications of FDA, offering a comprehensive overview of the subject.

Functional data can be viewed as smooth realizations of an underlying continuous stochastic process, where each observation is a functional time series. Therefore, each observation is intrinsically infinite dimensional. In FDA, functional principal component analysis (FPCA) plays a key role in dimensionality reduction. Shang (2014) provided a comprehensive review of FPCA, elucidating its applications in exploratory analysis, modeling, forecasting, and the classification of functional data. The development of FPCA can be dated back to the Karhunen-Loève decomposition (Karhunen, 1946). FPCA describes the stochastic evolution of the main characteristics associated with multiple systems and devices, where identifying the probability distribution of the principal component scores is important in characterizing the entire process. Some prominent works that implemented FPCA include Hall and Hosseini-Nasab (2005); Viviani et al. (2005); Hyndman and Ullah (2007); Di et al. (2009); Aue et al. (2015); Bongiorno and Goia (2019); Nie et al. (2018).

Most of the current FDA methodologies including FPCA have been developed with the assumption that the time dependence in the data is mild or negligible. However, many economic time series are time dependent, e.g. yield curves (Diebold and Li, 2006;

Hays et al., 2012), and intraday-price curves (Kokoszka et al., 2015). This is disadvantageous for dimensionality reduction in economic data where time dependence are well documented. In the context of FDA, functional data which are time-dependent are called functional time series (Horváth and Kokoszka, 2012). Dimensionality reduction techniques for functional time series data have been in development. Panaretos and Tavakoli (2013) proposed a Fourier analysis for stationary functional time series. Hörmann et al. (2015) proposed a dynamic functional principal component analysis (DFPCA). It is an extension of the dynamic principal component analysis (DPCA) proposed by Brillinger (2001) in a functional data framework. Some recent works which implemented DFPCA include Gao et al. (2019); Yang et al. (2022); Shang and Kearney (2022); Martínez-Hernández and Genton (2023).

On the other hand, many stationary and non-stationary functional time series in economics have also been modelled with dynamic factor models extensively. This is reflected in some recent works include Diebold and Li (2006); Hays et al. (2012); Liebl (2013); Kokoszka et al. (2015); Martínez-Hernández et al. (2022). In dynamic factor models, a large fraction of the variance in time series are explained by a smaller number of latent variables (Forni et al., 2000; Giannone et al., 2006). Some important works on dynamic factor models in stationary multivariate time series include Bai and Ng (2002); Forni et al. (2005); Lam et al. (2011). In the case of non-stationary multivariate time series, Stock and Watson (1988) investigated factors in co-integrated time series. Bai and Ng (2004) proposed a dynamic factor model for large dimensional and non-stationary panel data. Peña and Poncela (2006) proposed a procedure to build dynamic factor models for vector time series. In a more recent work closely related to dynamic factor models, Peña and Yohai (2016) proposed a generalized dynamic principal component analysis (GDPCA). It is a dimensionality reduction approach entirely based on data analytics. Smucler (2019) proved that when data follow a dynamic factor model with one dynamic factor, the first generalized dynamic principal component (GDPC) converges in mean square to the common part of the factor model.

In this paper, we develop and investigate the functional framework of Peña and Yohai (2016). The rest of the paper is organized as follows. In section 2, we describe the methodology of the proposed functional GDPCA (GDFPCA), the computation of functional GDPC (GDFPC), and consistency of FGDPC. In section 3, we show the results of Monte-Carlo studies with different data-generating processes that compare the GDFPCA with FPCA and DFPCA (Hörmann et al., 2015). In section 4, we apply GDFPCA on real data and compare the reconstructions with FPCA and DFPCA. Section 5 concludes with recommendations for future works.

2 Methodology

Consider n observations X_1, \dots, X_n of a functional time-series $(X_t, t \in \mathbb{Z})$, valued in $\mathcal{H} = \mathcal{L}^2(\mathcal{T})$, the space of complex square-integrable functions $(\int_{\mathcal{T}} f(u)\bar{f}(u)du, \bar{f}$ is the conjugate of f) on \mathcal{T} (a compact set in \mathbb{R}), with finite (Lebesgue-) measure. In practice, most applications are real-valued.

Let the inner product $\langle \cdot, \cdot \rangle : \mathcal{H} \times \mathcal{H} \rightarrow \mathbb{R}$, for $f, g \in \mathcal{H}$:

$$\langle f, g \rangle = \int_{\mathcal{T}} f(u) \bar{g}(u) du.$$

Then, \mathcal{H} is a Hilbert space with respect to the scalar product $\langle \cdot, \cdot \rangle$ with $\|f\|_{\mathcal{H}} = \langle f, f \rangle^{1/2}$ defining a norm.

A functional variable $X \in \mathcal{H}$ possesses a covariance operator $C := \mathbb{E}[(X - \mu) \otimes (X - \mu)]$ (where μ is the mean curve define by $\mu(t) = \mathbb{E}X(t)$ with $t \in \mathcal{T}$) with kernel $c(u, v) = \text{cov}(X(u), X(v))$ ($u, v \in \mathcal{T}$). Then, the integral operator C is defined by

$$(Cf)(u) = \int_{\mathcal{T}} c(u, v) f(v) dv, \quad f \in \mathcal{L}^2(\mathcal{T}), \quad u \in \mathcal{T}.$$

Suppose that each $(X_t, t \in \mathbb{Z})$ is a weakly stationary functional variable defined on some probability space (Ω, \mathcal{A}, P) :

- (i) $\mathbb{E}(X_t(u)) = \mathbb{E}(X_0(u)) = \mu(u)$, $u \in \mathcal{T}$,
- (ii) for all $h \in \mathbb{Z}$, and $u, v \in \mathcal{T}$; $c_h(u, v) := \text{Cov}(X_h(u), X_0(v)) = \text{Cov}(X_{t+h}(u), X_t(v))$.

We assume that

$$\sum_{h \in \mathbb{Z}} \left\{ \int_0^1 \int_0^1 |c_h(u, v)|^2 du dv \right\}^{1/2} < \infty,$$

ensuring that X_t has a spectral density.

This condition may e written in terms of the covariance operator C_h , $h \in \mathbb{Z}$ corresponding to c_h ($C_0 = C$).

The operator C admits an eigen-decomposition,

$$C(x) = \sum_{j=1}^{\infty} \lambda_j \langle x, \phi_j \rangle \phi_j,$$

where $\lambda_1 \geq \lambda_2 \geq \dots \geq 0$ are the eigenvalues of C and $\{\phi_j\}_{j \geq 1}$ the associated orthonormal eigenfunctions. This yields the Karhunen-Loève representation of X ,

$$X = \sum_{j=1}^{\infty} \lambda_j \langle X, \phi_j \rangle \phi_j.$$

This representation does not take into account the serial dependency on the functional time-series observations, X_t (Hörmann et al., 2015). Without a loss of generality let us assume that $(X_t, t \in \mathbb{Z})$ is centered.

Let us assume that the time series observations X_1, \dots, X_n follow the model below:

$$X_t(u) = Y_t(u) + e_t(u), \quad t = 1, \dots, n, \quad (1)$$

$$Y_t(u) = \sum_{h=0}^K f_{t-h} \beta_h(u),$$

where $\{\beta_h\}$ are factor loading curves, $\{f_t\}$ are scalar factor time series, $\{e_t\}$ is a sequence of centered independent and identically distributed (i.i.d) functional random variables in $\mathcal{L}^2(\mathcal{T})$. By assuming the orthonormality of the factor loading curves, we further assume the following:

Assumption A1. $\{e_t\}$ is uncorrelated with $\{Y_t\}$.

Assumption A2. Let $C_{Y,h}$ and C_e ($\{e_t\}$ is a white noise) be the covariance operators of $\{Y_t\}$ and $\{e_t\}$ respectively. Let $\lambda_j^{Y,h}$, λ_j^e be their respective ordered j th eigenvalues. Their maximum eigenvalues $\lambda_{max}^{Y,h}$ and λ_{max}^e are finite.

Motivated by the definition of multivariate GDPC (Peña and Yohai, 2016), we define the first FGDPC with K lags as a vector $\mathbf{f}^\top = (f_{1-K}, \dots, f_n)$, such that the reconstruction of the functional variable $X_t(\cdot)$ as a linear combination of $(f_{t-K}, \dots, f_{t-1}, f_t)$ is optimal with respect to the mean squared error (MSE) criterion. Specifically, given a $(n+K)$ -dimensional vector \mathbf{f} , a $(K+1)$ -dimensional vector of loading curves $\boldsymbol{\beta} = (\beta_0(u), \dots, \beta_K(u))^\top$ and a mean function $\alpha(u)$, the reconstruction of $X_t(\cdot)$ is defined as:

$$X_t^{R,b}(\mathbf{f}, \boldsymbol{\beta}, \alpha) = \alpha(u) + Y_t(u) = \alpha(u) + \sum_{h=0}^K f_{t-h} \beta_h(u), \quad (2)$$

where the superscripts R and b stand for reconstruction and backward respectively. The MSE loss function when we reconstruct the n functional time series using $\mathbf{f}, \boldsymbol{\beta}, \alpha$ is:

$$\text{MSE}(\mathbf{f}, \boldsymbol{\beta}, \alpha) = \frac{1}{n} \sum_{t=1}^n \left\| (X_t - X_t^{R,b}(\mathbf{f}, \boldsymbol{\beta}, \alpha)) \right\|_{\mathcal{H}}^2. \quad (3)$$

The values which minimize the above function is denoted as $(\hat{\mathbf{f}}, \hat{\boldsymbol{\beta}}, \hat{\alpha})$, is then the first FGDPC, and the second FGDPC is defined as the first FGDPC of the residuals:

$$r_t = X_t - X_t^{R,b}(\hat{\mathbf{f}}, \hat{\boldsymbol{\beta}}, \hat{\alpha}), \quad 1 \leq t \leq n, \quad (4)$$

and higher order FGDPC are defined similarly.

2.1 Truncated FGDPC

By letting $\{\phi_j\}$ be an orthonormal basis of $\mathcal{H} = \mathcal{L}^2(\mathcal{T})$, we expand the functional objects in equation (1):

$$X_t(u) = \sum_{j=1}^{\infty} \chi_{t,j} \phi_j(u); \beta_h(u) = \sum_{j=1}^{\infty} \beta_{h,j} \phi_j(u); e_t(u) = \sum_{j=1}^{\infty} \varepsilon_{t,j} \phi_j(u). \quad (5)$$

Then, equation (1) may be rewritten as:

$$\begin{aligned} \sum_{j=1}^{\infty} \chi_{t,j} \phi_j(u) &= Y_t(u) + \sum_{j=1}^{\infty} \varepsilon_{t,j} \phi_j(u), \quad t = 1, \dots, n, \\ Y_t(u) &= \sum_{h=0}^K \sum_{j=1}^{\infty} f_{t-h} \beta_{h,j} \phi_j(u). \end{aligned} \quad (6)$$

Let us consider a truncation of the previous equation,

$$X_t(u) \approx \sum_{j=1}^m \chi_{t,j} \phi_j(u) = \sum_{h=0}^K \sum_{j=1}^m f_{t-h} \beta_{h,j} \phi_j(u) + \sum_{j=1}^m \varepsilon_{t,j} \phi_j(u), \quad t = 1, \dots, n. \quad (7)$$

We assume the same truncated dimension $m = m_n = o(n)$ across h , m goes to ∞ with n . We derive the truncated reconstruction

$$X_t^{R,b}(\mathbf{f}, \boldsymbol{\beta}, \boldsymbol{\alpha}) \approx \sum_{h=0}^K \sum_{j=1}^m \alpha_j \phi_j(u) + \sum_{h=0}^K \sum_{j=1}^m f_{t-h} \beta_{h,j} \phi_j(u). \quad (8)$$

The target model can then be expressed as the dynamical factor model on the scores $\chi_{t,j}$

$$\chi_{t,j} = \sum_{h=0}^K \beta_{h,j} f_{t-h} + \varepsilon_{t,j}, \quad t = 1, \dots, n, \quad j = 1, \dots, m. \quad (9)$$

The parameters $\mathbf{f}, \boldsymbol{\beta}^m := (\beta_{h,j}) \in \mathbb{R}^{(K+1) \times m}$, $\boldsymbol{\alpha} = (\alpha_j) \in \mathbb{R}^m$ are estimated by minimizing the following least squares function:

$$\text{MSE}(\mathbf{f}, \boldsymbol{\beta}^m, \boldsymbol{\alpha}) = \frac{1}{nm} \sum_{t=1}^n \sum_{j=1}^m \left(\chi_{t,j} - \alpha_j + \sum_{h=0}^K f_{t-h} \beta_{h,j} \right)^2,$$

$$= \frac{1}{nm} \sum_{t=1}^n \left\| \chi_t - \chi_t^{R,b}(\mathbf{f}, \boldsymbol{\beta}^m, \boldsymbol{\alpha}) \right\|^2, \quad (10)$$

where $\chi_t^{R,b}(\mathbf{f}, \boldsymbol{\beta}^m, \boldsymbol{\alpha}) = \sum_{j=1}^m (\alpha_j + \sum_{h=0}^K f_{t-h} \beta_{h,j})$ is the multivariate GDPC (Peña and Yohai, 2016) for the vector $\chi_t = (\chi_{t,1}, \dots, \chi_{t,m})^\top$. The values $(\mathbf{f}, \boldsymbol{\beta}^m, \boldsymbol{\alpha})$ which minimize the above least squares function is denoted as $(\hat{\mathbf{f}}, \hat{\boldsymbol{\beta}}, \hat{\boldsymbol{\alpha}})$ and then

$$\chi_{t,j}^{R,b}(\hat{\mathbf{f}}, \hat{\boldsymbol{\beta}}^m, \hat{\boldsymbol{\alpha}}) = \hat{\alpha}_j + \sum_{h=0}^K \hat{f}_{t-h} \hat{\beta}_{h,j}, \quad j = 1, \dots, m. \quad (11)$$

The minimization of equation (3) can then be approximately solved by minimizing equation (10) based on the truncation of the functional objects $X_t(\cdot)$. Then the estimation of $(\mathbf{f}, \boldsymbol{\beta}, \boldsymbol{\alpha})$ is denoted $(\hat{\mathbf{f}}, \hat{\boldsymbol{\beta}}, \hat{\boldsymbol{\alpha}})$ with $\hat{\alpha}(u) = \sum_{j=1}^m \hat{\alpha}_j \phi_j(u)$, $\hat{\beta}_h(u) = \sum_{j=1}^m \hat{\beta}_{h,j} \phi_j(u)$. Then the estimated reconstruction of $X_t(\cdot)$ is

$$X_t^{R,b}(\hat{\mathbf{f}}, \hat{\boldsymbol{\beta}}, \hat{\boldsymbol{\alpha}}) = \hat{\alpha}(u) + \sum_{h=0}^K \hat{f}_{t-h} \hat{\beta}_h(u). \quad (12)$$

2.2 Computation of FGDPC

We see that the truncated $(\mathbf{f}, \boldsymbol{\beta}, \boldsymbol{\alpha})$ can be equivalently solved by minimizing the MSE loss function when we reconstruct the vector $\chi_t = (\chi_{t,1}, \dots, \chi_{t,m})^\top$. To compute $(\hat{\mathbf{f}}, \hat{\boldsymbol{\beta}}^m, \hat{\boldsymbol{\alpha}})$, we follow the approach in Peña and Yohai (2016). That is, given FGDPC \mathbf{f} , the coefficient matrix $\boldsymbol{\beta}^m$ and the vector $\boldsymbol{\alpha}$ can be readily computed using the least-squares method.

Differentiating (10) with respect to $\boldsymbol{\beta}_j^m$ and α_j leads to:

$$\begin{pmatrix} \boldsymbol{\beta}_j^m \\ \alpha_j \end{pmatrix} = (\mathbf{F}(\mathbf{f})^\top \mathbf{F}(\mathbf{f}))^{-1} \mathbf{F}(\mathbf{f})^\top \chi^j, \quad (13)$$

where $\boldsymbol{\beta}_j^m, j = 1, \dots, m$ are the rows of $\boldsymbol{\beta}^m$, $\chi^j = (\chi_{j,1}, \dots, \chi_{j,n})^\top$ and $\mathbf{F}(\mathbf{f})$ is a $n \times (K+2)$ matrix, with the t -th row $(f_t, f_{t+1}, \dots, f_{t+K}, 1)$. On the other hand, given $\boldsymbol{\beta}^m$ and $\boldsymbol{\alpha}$, \mathbf{f} can be computed by differentiating (10) with respect to \mathbf{f} . This leads to:

$$\begin{aligned} \mathbf{f} &= \mathbf{D}(\boldsymbol{\beta}^m)^{-1} \sum_{j=1}^m \mathbf{C}_j(\boldsymbol{\alpha}) \boldsymbol{\beta}_j^m, \\ \mathbf{C}_j(\boldsymbol{\alpha}_j) &= (c_{j,t,q}(\alpha_j))_{1 \leq t \leq n+K, 1 \leq q \leq K+1}, \end{aligned} \quad (14)$$

$c_{j,t,q}(\alpha_j) = (\chi_{j,t-q+1} - \alpha_j)$ when $1 \vee (t - n + 1) \leq q \leq (K + 1) \wedge t$ and zero otherwise. Furthermore,

$$\mathbf{D}(\beta^m) = \sum_{j=1}^m \mathbf{D}_j(\beta_j^m),$$

$$\mathbf{D}_j(\beta_j^m) = (d_{j,t,q}(\beta_j^m)),$$

where $(d_{j,t,q}(\beta_j^m))$ is a $(n + K) \times (n + K)$ matrix given by,

$$(d_{j,t,q}(\beta_j^m)) = \sum_{v=(t-K) \vee 1}^{t \wedge T} \beta_{j,q-v+1}^m \beta_{j,t-v+1}^m,$$

when $(t - K) \vee 1 \leq q \leq (t + K) \wedge (n + K)$ and zero otherwise. Given an initial value of the first FGDPC, $\mathbf{f}^{(0)}$, $(\hat{\mathbf{f}}, \hat{\beta}^m, \hat{\alpha})$ can be computed with a two-step iterative process based on equations (13) and (14):

Step 1: Based on (13), define $\beta_j^{m(h)}$ and $\alpha_j^{(h)}$, for $1 \leq j \leq m$,

$$\begin{pmatrix} \beta_j^{m(h)} \\ \alpha_j^{(h)} \end{pmatrix} = (\mathbf{F}(\mathbf{f}^{(h)})^\top \mathbf{F}(\mathbf{f}^{(h)})^{-1} \mathbf{F}(\mathbf{f}^{(h)})^\top \chi^j.$$

Step 2: Based on (14), define $\mathbf{f}^{(h+1)}$ by,

$$\begin{aligned} \mathbf{f}^* &= \mathbf{D}(\beta^{m(h)})^{-1} \mathbf{C}(\alpha^{(h)}) \beta^{m(h)}, \\ \mathbf{f}^{(h+1)} &= (n + K - 1)^{1/2} (\mathbf{f}^* - \bar{\mathbf{f}}^*) / \|\mathbf{f}^* - \bar{\mathbf{f}}^*\|, \end{aligned} \quad (15)$$

where $\bar{\mathbf{f}}^*$ is the mean of \mathbf{f}^* . The two-step iterations is stopped when

$$\frac{\text{MSE}(\mathbf{f}^{(h)}, \beta^{m(h)}, \alpha^{(h)}) - \text{MSE}(\mathbf{f}^{(h+1)}, \beta^{m(h+1)}, \alpha^{(h+1)})}{\text{MSE}(\mathbf{f}^{(h)}, \beta^{m(h)}, \alpha^{(h)})} < \epsilon, \quad (16)$$

where ϵ is some value.

2.3 Consistency of FGDPC

Let $\psi_t^m = (\beta^m)^\top F_t$. It is readily shown with Theorem 1 from [Smucler \(2019\)](#) that the $\chi_t^{R,b}(\hat{\mathbf{f}}, \hat{\beta}^m, \hat{\alpha})$ converges in mean square to ψ_t^m and χ_t under the following assumptions A3 to A7 ([Smucler, 2019](#)). With this result, we also prove the mean-square convergence of $X_t^{R,b}(\hat{\mathbf{f}}, \hat{\beta}, \hat{\alpha})$ to the common part of the functional factor model Y_t and X_t . Throughout this section, we let $\chi, \hat{\chi}, \mathcal{E}, \Psi, \hat{F}, F$ be the matrices with rows $\chi_t^\top, \chi_t^{R,b}(\hat{\mathbf{f}}, \hat{\beta}^m, \hat{\alpha})^\top, \varepsilon_t^\top, (\psi_t^m)^\top, \hat{F}_t^\top$, and F_t^\top , $t = 1, \dots, n$ respectively.

Assumption A3. ψ_t^m and $\varepsilon_t = (\varepsilon_{t,1}, \dots, \varepsilon_{t,m})$ represents a zero-mean, second order m -dimensional stationary process that has a spectral density.

Assumption A4. F_t is a second order stationary process. F_t and ε_t are uncorrelated for all t ; Let $\Sigma^\chi, \Sigma^\varepsilon$ be the covariance matrices of χ_t and ε_t each with finite maximum of the eigenvalues.

Assumption A5. $\lim_{n \rightarrow \infty} \beta^m (\beta^m)^\top / m = S$, where S is positive definite.

Assumption A6. $\limsup_m \sum_{u \in \mathbb{Z}} [E\{\varepsilon_t^\top \varepsilon_{t+u}\} / m]^2 < \infty$.

Assumption A7. $\limsup_m (1/m) \sup_{t,s \in \mathbb{Z}} \sum_{j=1}^m \sum_{i=1}^m |\text{cov}(\varepsilon_{t,i} \varepsilon_{s,i}, \varepsilon_{t,j} \varepsilon_{s,j})| < \infty$.

Assumption A8. $\sum_{j>m} \chi_{t,j}^2 = O(m^{-2\tau})$, $\tau > 1$.

Assumptions **A3** to **A7** are similar to the assumptions used by [Stock and Watson \(2002\)](#); [Smucler \(2019\)](#). Assumptions **A3** and **A4** ensure the uniqueness of the decomposition, $\chi_t = \psi_t^m + \varepsilon_t$ ([Forni et al., 2015](#)). Assumption **A5** is a standard assumption in ordinary least square estimation. Assumption **A6** allows for serial correlations in ε_t , and assumption **A7** constrains the size of fourth moments of ε_t ([Stock and Watson, 2002](#)). Assumption **A8** may be fulfilled when using orthogonal polynomials or Fourier functions and smooth condition of the functional objects. For instance, if β_h is τ -times continuously differentiable function with respect to m suitable basis functions is of an order of at most $m^{-2\tau}$.

Theorem 1. Assume that A3-A7 hold. Let the common part of a dynamic factor model be defined by $\psi_t^m = (\beta^m)^\top F_t$, where $\beta^m := (\beta_{h,j}) \in \mathbb{R}^{(K+1) \times m}$ and $F_t = (f_t, \dots, f_{t-K})^\top$. Secondly, let $\chi_t^{R,b}(\hat{\mathbf{f}}, \hat{\beta}^m, \hat{\alpha})$ be the reconstruction of χ_t with the estimated $(\hat{\mathbf{f}}, \hat{\beta}^m, \hat{\alpha})$. Then, as $n \rightarrow \infty$ and $m \rightarrow \infty$,

$$\frac{1}{nm} \sum_{t=1}^n \left\| \psi_t^m - \chi_t^{R,b}(\hat{\mathbf{f}}, \hat{\beta}^m, \hat{\alpha}) \right\|^2 = O_P \left(\frac{1}{m^{1/4}} \right), \quad (17)$$

$$\frac{1}{nm} \sum_{t=1}^n \left\| \chi_t - \chi_t^{R,b}(\hat{\mathbf{f}}, \hat{\beta}^m, \hat{\alpha}) \right\|^2 = O_P \left(\frac{1}{m^{1/2}} \right). \quad (18)$$

In the following theorem we give an asymptotic result on the functional reconstruction.

Theorem 2. Assume that A1-A8 hold. Let the common part of a functional dynamic factor model be defined by $Y_t = (\beta)^\top F_t$, where $\beta := (\beta_0(\cdot), \dots, \beta_K(\cdot))$ is a vector of $K+1$ factor loading curves and $F_t = (f_t, \dots, f_{t-K})^\top$. Secondly, let $X_t^{R,b}(\hat{\mathbf{f}}, \hat{\beta}, \hat{\alpha})$ be the reconstruction of X_t with the estimated $(\hat{\mathbf{f}}, \hat{\beta}, \hat{\alpha})$. Then, as $n \rightarrow \infty$ and $m \rightarrow \infty$,

$$\frac{1}{nm} \sum_{t=1}^n \left\| X_t - X_t^{R,b}(\hat{\mathbf{f}}, \hat{\beta}, \hat{\alpha}) \right\|_{\mathcal{H}}^2 = O_P \left(\frac{1}{m^{1/2}} \right). \quad (19)$$

The proofs of Theorem 1 and Theorem 2 are in Appendix A.

3 Simulation Studies

We perform simulation studies to compare the performance of GDFPCA with that of FPCA and DFPCA using three data-generating processes, i.e. the first order functional autoregressive process (FAR(1)), a smoothed first order vector autoregressive integrated(1) process (VAR(1,1)), and a dynamic factor model. The idea is to assess the performance of GDPCA on data generated from a stationary model, FAR(1); a non-stationary model, VAR(1,1); and a dynamic factor model.

In each simulated functional time series, we compute the PC scores for all three frameworks of PCA, and reconstruct the series using the computed PC scores for all three frameworks of PCA. The number of principal components (PC), p is chosen such that the explained variance by GDFPCA in all cases are at least 80%. For all cases, the simulation is repeated for 50 iterations. We evaluate the performances of all reconstructions based on the mean squared error (MSE) and variance explained.

3.1 Simulation results in a stationary case: First order functional autoregressive process (FAR(1))

We generate the FAR(1) process: $X_{n+1} = \psi(X_n) + \epsilon_{n+1}$ with the `fts.rar` function in the package `freqdom.fda` (Hörmann et al., 2015). In `fts.rar`, the simulation process of FAR(1) was performed in a finite dimension d :

$$\begin{aligned} \langle X_{n+1}, v_j \rangle &= \langle \psi(X_n), v_j \rangle + \langle \epsilon_{n+1}, v_j \rangle \\ &= \langle \psi(\sum_{i=1}^{\infty} \langle X_n, v_i \rangle v_i), v_j \rangle + \langle \epsilon_{n+1}, v_j \rangle \\ &\approx \sum_{i=1}^d \langle X_n, v_i \rangle \langle \psi(v_i), v_j \rangle + \langle \epsilon_{n+1}, v_j \rangle, \end{aligned} \quad (20)$$

where $(v_i), i \in \mathbf{N}$ are the Fourier basis functions on $[0,1]$. By letting $\mathbf{X}_n = (\langle X_n, v_1 \rangle, \dots, \langle X_n, v_d \rangle)'$ and $\boldsymbol{\epsilon}_n = (\langle \epsilon_{n+1}, v_1 \rangle, \dots, \langle \epsilon_{n+1}, v_d \rangle)'$, the first d Fourier coefficients of X_n can be approximated as a VAR(1) equation $\mathbf{X}_{n+1} = \mathbf{B}\mathbf{X}_n + \boldsymbol{\epsilon}_n$, where $\mathbf{B} = (\langle \psi(v_i), v_j \rangle : 1 \leq i, j \leq d)$ (Hörmann et al., 2015). We use the default option of $\mathbf{B} = \kappa \mathbf{G}/2\|\mathbf{G}\|$ where $\mathbf{G}_{ij} = \exp(-(i+j))$ where $\mathbf{G}_{ij} \rightarrow 0$ as $i, j \rightarrow \infty$.

We consider the settings where $d = 15, 31, 45$, $\kappa = 0.3, 0.6, 0.9$ and the number of observations, $n = 300$. The selection of d is made to comply with the odd-number requirement for the number of Fourier basis functions. The value of n was chosen based on the observation that all values beyond 300 exhibit similar performance. In all settings, a higher number of PC is required to achieve at least 80% of the explained variance for the simulated time series as κ increases. We find that $p = 7, 10, 15$ is sufficient for settings with $\kappa = 0.3, 0.6, 0.9$ respectively.

The boxplots of the distribution of MSE for three frameworks of PCA are illustrated in Figure 1. The boxplots of the distribution of explained variance for three frameworks of PCA are illustrated in Figure 2. When d and κ are small, the performance of GDFPCA is similar to that of DFPCA and better than the performance of FPCA. As d and κ increase, GDFPCA outperforms its counterparts.

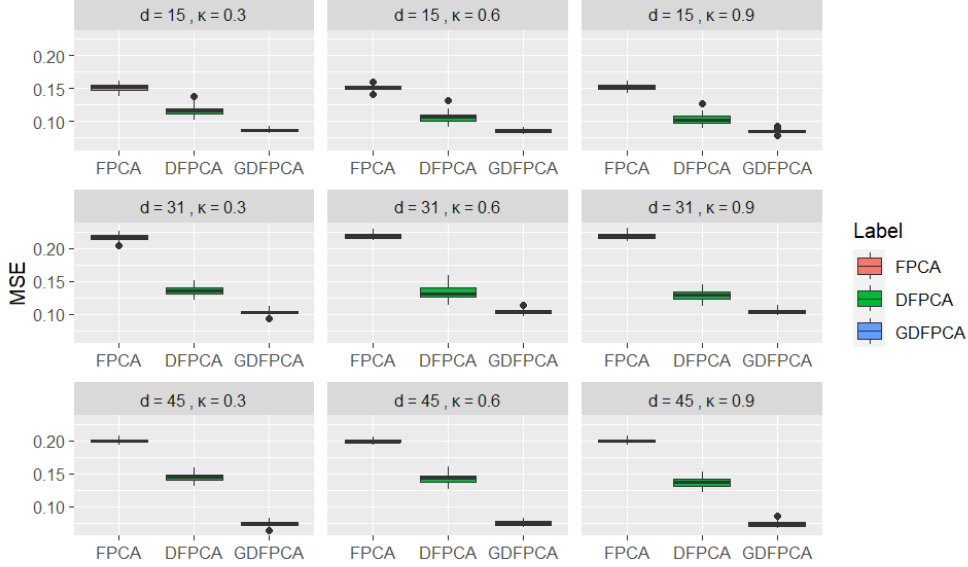


Fig. 1: Boxplots of MSE of 50 iterations of simulated stationary FAR(1) processes.

3.2 Simulation results in an non-stationary case: Smoothed VARI(1,1) process

We consider a non-stationary smoothed VARI(1,1) process. We follow the approach of Peña and Yohai (2016) to generate a vector autoregressive integrated process of order one. A VARI(1,1) m -dimensional vector series $\mathbf{z}_t, t = 1, \dots, T$ is generated as follows:

$$\begin{aligned}\mathbf{z}_t &= \mathbf{z}_{t-1} + \mathbf{x}_t, \\ \mathbf{x}_t &= A\mathbf{x}_{t-1} + \mathbf{u}_t,\end{aligned}$$

where \mathbf{u}_t are i.i.d m -dimensional vectors with distribution $\mathbf{N}_m(0, \mathbf{I})$. A is generated with $A = V\Lambda V'$ where V is an orthogonal matrix generated randomly with an uniform distribution and Λ is a diagonal matrix, where the diagonal elements are generated from an uniform distribution $\mathbf{U}[0, 0.9]$. Once we generate the m -dimensional VARI(1,1) process, they are smoothed with 21 Fourier basis functions; we found that it is adequate for the computation. We consider $m = 50, 75, 100$ and time $T = 100, 150, 200$.

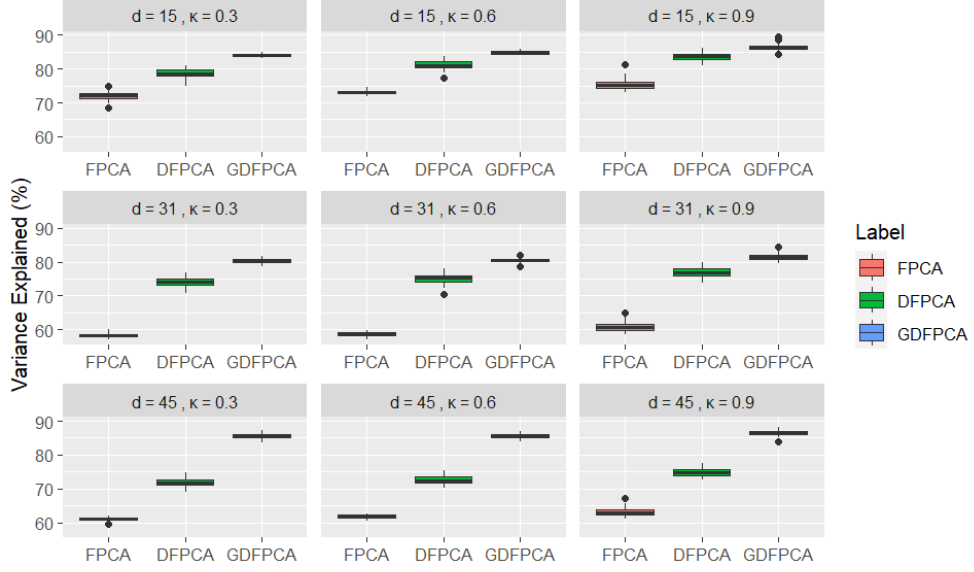


Fig. 2: Boxplots of explained variance of 50 iterations of a simulated FAR(1) process.

$p = 2$ is sufficient to account for the explained variance threshold of 80%. The boxplots of the distribution of MSE for three frameworks of PCA are illustrated in Figure 3. The boxplots of the distribution of explained variance for three frameworks of PCA are illustrated in Figure 4. In line with previous observations, GDFPCA consistently outperforms its counterparts by demonstrating the lowest MSE and the highest explained variance across all settings.

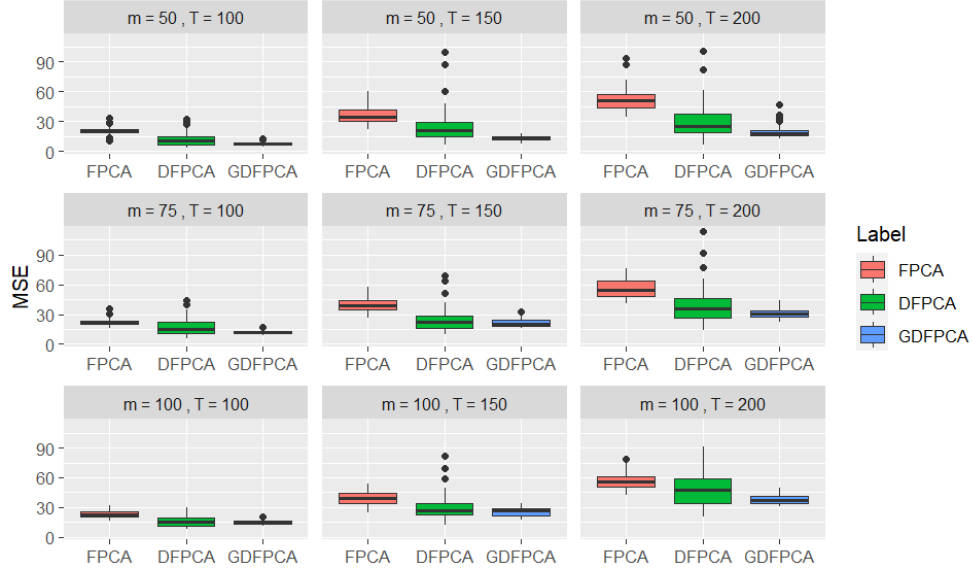


Fig. 3: Boxplots of MSE of 50 iterations of simulated smoothed VARI(1,1) processes.

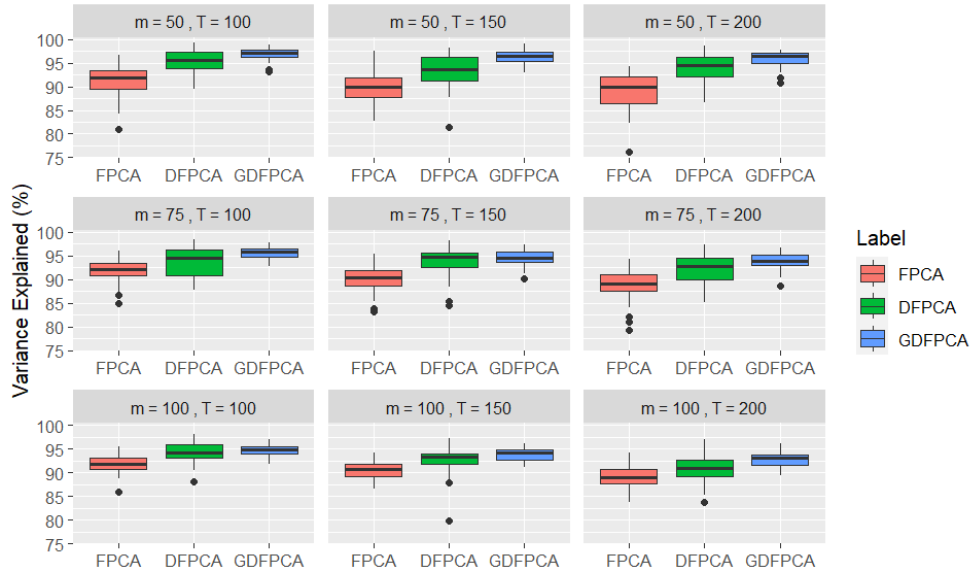


Fig. 4: Boxplots of explained variance of 50 iterations of simulated smoothed VARI(1,1) processes.

3.3 Simulation results using the dynamic factor model

In this section, we consider a dynamic factor model with a static factor representation (Forni et al., 2009):

$$z_{it} = \lambda_{i1}F_{1t} + \lambda_{i2}F_{2t} + \dots + \lambda_{ir}F_{rt} + \epsilon_{it}, \quad i = 1, \dots, m, \quad t = 1, \dots, T,$$

$$\mathbf{F}_t = \mathbf{D}\mathbf{F}_{t-1} + \mathbf{K}\mathbf{u}_t,$$

where $\mathbf{F}_t = (F_{1t}, F_{2t}, \dots, F_{rt})'$ and $\mathbf{u}_t = (u_{1t}, u_{2t}, \dots, u_{qt})'$, \mathbf{D} is an $r \times r$ matrix and \mathbf{K} is an $r \times q$ matrix respectively. u_{jt} and ϵ_{it} are i.i.d. standard normal random variables. λ_{hi} and the entries of \mathbf{K} are generated based on an independent and uniform distribution on the interval $(-1,1)$, $U(-1,1)$. Furthermore, the entries of \mathbf{D} are generated according to section 4.1 in (Forni et al., 2017). Firstly, each entry of \mathbf{D} is generated based on an independent $U(-1,1)$. Second, the resulting matrix from the first step is divided by its spectral norm to obtain unit norm. Lastly, we multiply the resulting matrix by a random variable generated from $U(-1,1)$.

The simulation results indicate that $p = 6$ is sufficient for the explained variance to account for at least 80% for all frameworks of PCA. The boxplots of the distribution of MSE for the reconstructions using three frameworks of PCA are illustrated in Figure 5. The boxplots of the distribution of explained variance for three frameworks of PCA are illustrated in Figure 6. Similarly, GDFPCA outperforms its counterpart by having the lowest MSE and highest explained variance.

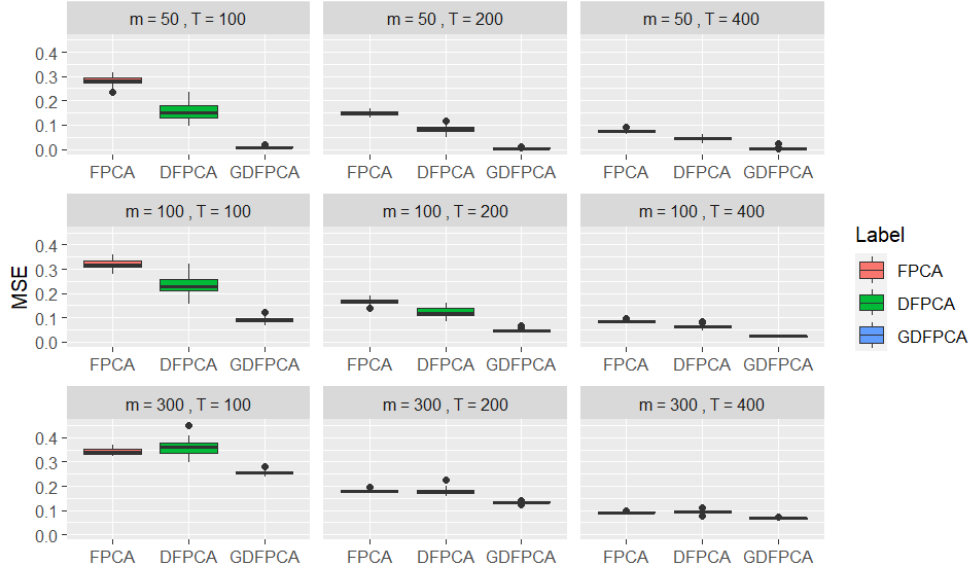


Fig. 5: Boxplots of MSE of 50 iterations of a simulated dynamic factor model.



Fig. 6: Boxplots of explained variance of 50 iterations of a simulated dynamic factor model.

4 Applications to real data

4.1 Particles with a diameter of 10 micrometers or less (PM10)

In this example, we perform the GDFPCA on the PM10 dataset available in the R package `freqdom.fda` (Hormann and Kidzinski, 2022). This dataset consists of half-hourly measurements of particulate-matter concentration with an aerodynamic diameter of less than $10\mu\text{m}$, in ambient air taken in Graz, Austria from the period of October 1, 2010 to March 31, 2011. The data was already pre-transformed from discrete data to functional data using 15 Fourier basis functions.

Figure 7 show the plot of 175 daily curves in the PM10 data set. Similarly, we also perform the FPCA and DFPCA on the data set. The percentage of the explained variance by three frameworks of PCA are reported in Table 1.

We observe that the reconstruction using GDFPCA accounts for a similar percentage of explained variance to that of DFPCA. Both reconstructions using GDFPCA and DFPCA perform better than that of FPCA. This is true for all p from 1 to 3.

4.2 Standard&Poor's 100 index (S&P100)

We first applied the GDFPCA on 100 stocks in the S&P100 as of September 2023. The daily closing prices from January 1 2020 to January 2021 were acquired from <http://www.investing.com>, and the log-returns of the daily closing prices were calculated before performing the GDFPCA. Since the stocks have a wide range of variation,

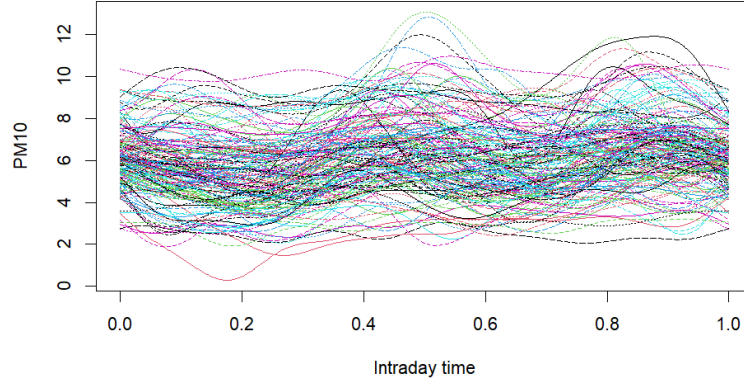


Fig. 7: A plot of the data set PM10 in the form of functional time series.

Type of PCA	Accumulated percentage of variance explained		
	No. of PC = 1	No. of PC = 2	No. of PC = 3
FPCA	72.3%	82.6%	88.7%
DFPCA	82.6%	91.8%	94.7%
GDFPCA	81.1%	89.7%	93.8%

Table 1: Empirical variance of the data set PM10 explained by three frameworks of PCA.

we performed scaling and centering on the data before smoothing the data. We then applied the GDFPCA on the data. In addition to GDFPCA, we also performed the FPCA and DFPCA on the data. The percentage of the variance explained by all three frameworks of PCA are reported in Table 2. Figure 8 shows the plot of 100 stocks in the form of functional time series.

We observe that the reconstruction using GDFPCA accounts for a similar percentage of explained variance to that of FPCA. Both reconstructions using GDFPCA and FPCA perform better than that of DFPCA. This is true for all p from 1 to 3. For $p = 3$, GDFPCA has the highest percentage of the explained variance. This is expected as the data exhibits non-stationarity, and DFPCA requires stationarity in the data (Hörmann et al., 2015).

4.3 Trading Volume of Bitcoin

In this section, we compare the performance of three frameworks of PCA on hourly trading volume of Bitcoin in 2021. The data are acquired from <http://www.bitstamp.net>. The data is arranged in a 24 x 365 matrix where each row represents an hour, each column represents a day. Figure 9 shows the plot of the smoothed trading volume of

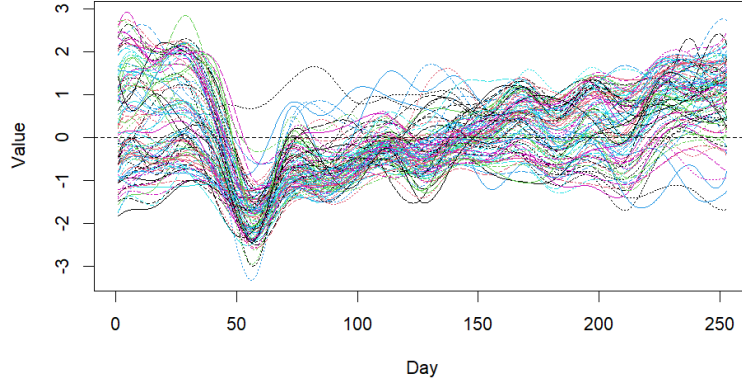


Fig. 8: A plot of the centered, scaled and smoothed time series of the 100 stocks in S&P100.

Type of PCA	Accumulated percentage of variance explained		
	No. of PC = 1	No. of PC = 2	No. of PC = 3
FPCA	73.8%	81.7%	85.6%
DFPCA	37.9%	56.1%	80.5%
GDFPCA	78.5%	86.8%	91.5%

Table 2: Variance of the stocks in S&P100 explained by three frameworks of PCA.

Bitcoin. The percentage of empirical variance explained by three frameworks of PCA are reported in Table 3.

The results indicate that the reconstruction using DFPCA accounts for the highest percentage when $p = 1$. However, as p increases, the improvements in explained variance are higher for GDFPCA.

Type of PCA	Accumulated percentage of variance explained			
	No. of PC = 1	No. of PC = 2	No. of PC = 3	No. of PC = 4
FPCA	49.6%	61.7%	70.7%	78.7%
DFPCA	64.3%	76.3%	82.7%	85.7%
GDFPCA	60.2%	75.2%	83.1%	87.9%

Table 3: Empirical variance of the trading volume of Bitcoin explained by three frameworks of PCA.

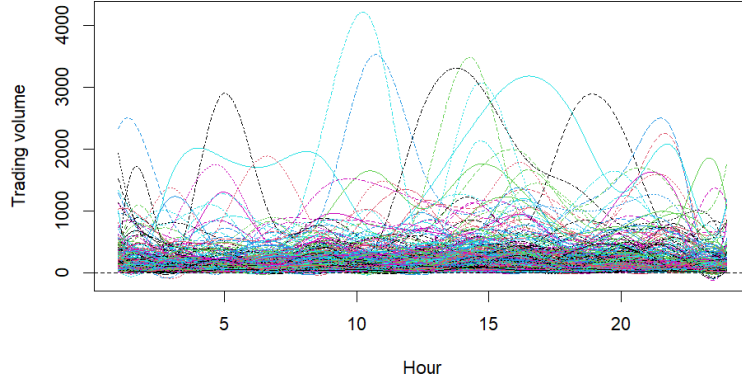


Fig. 9: (a) A plot of the trading volumes of BTC in the form of functional time series.

5 Conclusions

We proposed a functional framework of GDFPCA (Peña and Yohai, 2016) which represents a data analytic approach to dimension reduction in functional time series. We define the reconstruction of the original functional time series using GDPC via a truncation of the functional dynamic factor model.

The outcomes of three simulation studies with data-generating processes suggested that reconstructions of original functional time series by GDFPCA and DFPCA are comparable based on the explained variance by both frameworks when the data generating process is stationary. On the other hand, when the data-generating process is non-stationary, GDFPCA surpasses both DFPCA and FPCA.

The results the applications to real data reaffirm the findings in the simulations studies. This implies that GDFPCA is versatile for dimension reduction in various types of functional data regardless of the stationarity of the dataset.

The use of GDFPCA can be extended to enhance the prediction of both stationary and non-stationary functional time series models. Most works available in the literature tend to focus on the stationary framework of functional time series models (Aue et al., 2015; Shang and Kearney, 2022), yet GDFPCA is hoped to contribute to the non-stationary time series aspect.

Appendix A

These proofs of Lemma 1 and Theorem 1 follow the same general strategy of that of Smucler (2019). For the purpose of completeness, we outline the main steps of the proofs of Lemma 1 and Theorem 1 as follows:

Lemma 1: Assume A6 and A7 hold, then,

$$\frac{\|\mathcal{E}\|}{\sqrt{nm}} = O_P\left(\frac{1}{m^{1/4}}\right)$$

Proof of Lemma 1. Consider $v \in \mathbb{R}^m$ with $\|v\| = 1$, then using Cauchy-Schwarz inequality we get:

$$\frac{v^T \mathcal{E}^T \mathcal{E} v}{nm} \leq \left(\frac{1}{m^2} \sum_{i,j=1}^m \left(\frac{1}{n} \sum_{t=1}^n \varepsilon_{t,i} \varepsilon_{t,j} \right)^2 \right)^{1/2}.$$

Thus we have:

$$\left(\frac{\|\mathcal{E}\|^2}{nm} \right)^2 = \left(\sup_{\|v\|=1} \frac{v^T \mathcal{E}^T \mathcal{E} v}{nm} \right)^2 \leq \frac{1}{m^2} \sum_{i,j=1}^m \left(\frac{1}{n} \sum_{t=1}^n \varepsilon_{t,i} \varepsilon_{t,j} \right)^2.$$

Using A6 and A7 we finally get:

$$\left(\frac{\|\mathcal{E}\|}{\sqrt{nm}} \right)^4 = O_P\left(\frac{1}{m}\right).$$

□

Proof of Theorem 1. We have:

$$\begin{aligned} \frac{1}{nm} \sum_{t=1}^n \left\| \chi_t - \chi_t^{R,b}(\hat{\mathbf{f}}, \hat{\boldsymbol{\beta}}^m, \hat{\boldsymbol{\alpha}}) \right\|^2 &\leq \frac{1}{nm} \sum_{t=1}^n \left\| \psi_t^m + \varepsilon_t - \chi_t^{R,b}(\hat{\mathbf{f}}, \hat{\boldsymbol{\beta}}^m, 0) \right\|^2 \\ &= \frac{1}{nm} \sum_{t=1}^n \sum_{j=1}^m \varepsilon_{t,j}^2 \\ &= \frac{\|\mathcal{E}\|^2}{nm}, \end{aligned} \tag{A1}$$

then, as $m = o(n)$ we get from Lemma 1:

$$\frac{1}{nm} \sum_{t=1}^n \left\| \chi_t - \chi_t^{R,b}(\hat{\mathbf{f}}, \hat{\boldsymbol{\beta}}^m, \hat{\boldsymbol{\alpha}}) \right\|^2 = O_P\left(\frac{1}{m^{1/2}}\right).$$

Notice that,

$$\begin{aligned} \frac{1}{nm} \sum_{t=1}^n \left\| \chi_t - \chi_t^{R,b}(\hat{\mathbf{f}}, \hat{\boldsymbol{\beta}}^m, \hat{\boldsymbol{\alpha}}) \right\|^2 &= \frac{1}{nm} \sum_{t=1}^n \sum_{j=1}^m \varepsilon_{t,j}^2 + \frac{1}{nm} \sum_{t=1}^n \left\| \psi_t^m - \chi_t^{R,b}(\hat{\mathbf{f}}, \hat{\boldsymbol{\beta}}^m, \hat{\boldsymbol{\alpha}}) \right\|^2 \\ &\quad - \frac{2\langle \mathcal{E}, \hat{\chi} - \Psi \rangle}{nm}. \end{aligned} \quad (\text{A2})$$

By combining (A1) and (A2), we get:

$$\frac{1}{nm} \sum_{t=1}^n \left\| \psi_t^m - \chi_t^{R,b}(\hat{\mathbf{f}}, \hat{\boldsymbol{\beta}}^m, \hat{\boldsymbol{\alpha}}) \right\|^2 \leq \frac{2\langle \mathcal{E}, \hat{\chi} - \Psi \rangle}{nm}.$$

Then, it is sufficient to prove that:

$$\frac{2\langle \mathcal{E}, \hat{\chi} - \Psi \rangle}{nm} = O_P\left(\frac{1}{m^{1/4}}\right), \quad (\text{A3})$$

Since $\chi_t^\top = (\beta^m)^\top F_t + \varepsilon_t^\top$, an application of triangular inequality on the corresponding matrices implies that $\|\chi\| \leq \|\beta^m\| \|F\| + \|\mathcal{E}\|$. Assumption A5 implies that $\|\beta^m\| = O(m^{1/2})$, and F_t is second-order stationary, we have $\|F\| = O_P(n^{1/2})$. By Lemma 1, $\|\chi\| = O_P((nm)^{1/2})$ and $\|\Psi\| = O_P((nm)^{1/2})$. Since $\hat{\chi}$ is obtained by projecting χ on the space generated by the columns of F_t and the vector with n coordinates all equal to 1, $\|\hat{\chi}\| \leq \|\chi\|$. Both Ψ and $\hat{\chi}$ have rank bounded by $r = k + 2$. Hence, it is enough to prove that for each fixed $C_1 > 0$,

$$\sup_{\|L\| \leq (nm)^{1/2} C_1, \text{rank} \leq r} \left| \frac{\langle \mathcal{E}, L \rangle}{nm} \right| = O_P\left(\frac{1}{m^{1/4}}\right).$$

We take L with $\|L\| \leq (Tm)^{1/2} C_1$, and $\text{rank}(L) \leq r$. Using the Singular Value Decomposition, we write $L = \sum_{l=1}^r \sigma_l u_l v_l^\top$, with u_l and v_l having unit norm. Then,

$$\begin{aligned} \left| \frac{\langle \mathcal{E}, L \rangle}{nm} \right| &\leq \frac{1}{nm} \sum_{l=1}^r \sigma_l |\langle \mathcal{E}, u_l v_l \rangle| \leq \frac{1}{nm} \max_{l \leq r} \sigma_l \sum_{l=1}^r |\langle \mathcal{E}, u_l v_l \rangle| \\ &= \frac{1}{nm} \|L\| \sum_{l=1}^r |\langle \mathcal{E}, u_l v_l \rangle|. \end{aligned}$$

Take any $u \in \mathbb{R}^T, v \in \mathbb{R}^m$ with unit norm. By using the cyclic property of the trace, $|\langle \mathcal{E}, uv^\top \rangle| = |\text{tr}(uv^\top \mathcal{E})| = |\text{tr}(u^\top \mathcal{E} v)| \leq \|\mathcal{E}\|$. With Lemma 1, we get:

$$\left| \frac{\langle \mathcal{E}, L \rangle}{nm} \right| \leq \frac{r \|\mathcal{E}\| \|L\|}{nm} \leq \frac{r \|\mathcal{E}\| C_1}{(nm)^{1/2}} = O_P\left(\frac{1}{m^{1/4}}\right).$$

Thus, by combining (A1), (A2), (A3), and $m = o(n)$ we get:

$$\frac{1}{nm} \sum_{t=1}^n \left\| \psi_t^m - \chi_t^{R,b}(\hat{\mathbf{f}}, \hat{\boldsymbol{\beta}}^m, \hat{\boldsymbol{\alpha}}) \right\|^2 = O_P \left(\frac{1}{m^{1/4}} \right). \quad (\text{A4})$$

□

Proof of Theorem 2. Recall that $\{\phi_j\}$ are the eigenbasis used to expand the functional variables:

$$X_t(u) = \sum_{j \geq 1} \chi_{t,j} \phi_j(u), \quad X_t^{R,b}(u) = \sum_{j=1}^m \chi_{t,j}^{R,f} \phi_j(u).$$

Let $X_t^{R,b}(\hat{\mathbf{f}}, \hat{\boldsymbol{\beta}}, \hat{\boldsymbol{\alpha}})$ be denoted here $X_t^{R,b}$ for simplicity of notation. Then, we have

$$\begin{aligned} \frac{1}{nm} \sum_{t=1}^n \left\| X_t - X_t^{R,b}(\hat{\mathbf{f}}, \hat{\boldsymbol{\beta}}, \hat{\boldsymbol{\alpha}}) \right\|_{\mathcal{H}}^2 &= \frac{1}{nm} \sum_{t=1}^n (\chi_t - \chi_t^{R,f})^\top (\chi_t - \chi_t^{R,f}) + \frac{1}{nm} \sum_{t=1}^n \sum_{j>m} (\chi_{t,j})^2 \\ &= \frac{1}{nm} \sum_{t=1}^n \left\| \chi_t - \chi_t^{R,f} \right\|^2 + o \left(\frac{1}{nm^{1+2\tau}} \right) \end{aligned}$$

This fulfills the proof by the help of Theorem 1. □

References

- Aue, A., Norinho, D.D., Hörmann, S.: On the prediction of stationary functional time series. *Journal of the American Statistical Association* **110**(509), 378–392 (2015)
- Bongiorno, E.G., Goia, A.: Describing the concentration of income populations by functional principal component analysis on lorenz curves. *Journal of Multivariate Analysis* **170**, 10–24 (2019)
- Bai, J., Ng, S.: Determining the number of factors in approximate factor models. *Econometrica* **70**(1), 191–221 (2002)
- Bai, J., Ng, S.: A panic attack on unit roots and cointegration. *Econometrica* **72**(4), 1127–1177 (2004)
- Brillinger, D.R.: Time series: Data analysis and theory. Society for Industrial and Applied Mathematics (2001)
- Di, C.-Z., Crainiceanu, C.M., Caffo, B.S., Punjabi, N.M.: Multilevel functional principal component analysis. *The annals of applied statistics* **3**(1), 458 (2009)
- Diebold, F.X., Li, C.: Forecasting the term structure of government bond yields. *Journal of econometrics* **130**(2), 337–364 (2006)
- Forni, M., Giannone, D., Lippi, M., Reichlin, L.: Opening the black box: Structural factor models with large cross sections. *Econometric Theory* **25**(5), 1319–1347 (2009)
- Forni, M., Hallin, M., Lippi, M., Reichlin, L.: The generalized dynamic-factor model: Identification and estimation. *Review of Economics and statistics* **82**(4), 540–554 (2000)
- Forni, M., Hallin, M., Lippi, M., Reichlin, L.: The generalized dynamic factor model: one-sided estimation and forecasting. *Journal of the American statistical association* **100**(471), 830–840 (2005)
- Forni, M., Hallin, M., Lippi, M., Zaffaroni, P.: Dynamic factor models with infinite-dimensional factor spaces: One-sided representations. *Journal of econometrics* **185**(2), 359–371 (2015)
- Forni, M., Hallin, M., Lippi, M., Zaffaroni, P.: Dynamic factor models with infinite-dimensional factor space: Asymptotic analysis. *Journal of Econometrics* **199**(1), 74–92 (2017)
- Giannone, D., Reichlin, L., Sala, L.: Vars, common factors and the empirical validation of equilibrium business cycle models. *Journal of Econometrics* **132**(1), 257–279 (2006)

- Gao, Y., Shang, H.L., Yang, Y.: High-dimensional functional time series forecasting: An application to age-specific mortality rates. *Journal of Multivariate Analysis* **170**, 232–243 (2019)
- Hall, P., Hosseini-Nasab, M.: On Properties of Functional Principal Components Analysis. *Journal of the Royal Statistical Society Series B: Statistical Methodology* **68**(1), 109–126 (2005)
- Horváth, L., Kokoszka, P.: Inference for functional data with applications. Springer Science & Business Media **200** (2012)
- Hormann, S., Kidzinski, L.: Freqdom.fda: Functional Time Series: Dynamic Functional Principal Components. (2022). R package version 1.0.1. <https://CRAN.R-project.org/package=freqdom.fda>
- Hörmann, S., Kidziński, L., Hallin, M.: Dynamic functional principal components. *Journal of the Royal Statistical Society Series B: Statistical Methodology* **77**(2), 319–348 (2015)
- Hays, S., Shen, H., Huang, J.Z.: Functional dynamic factor models with application to yield curve forecasting. *The Annals of Applied Statistics*, 870–894 (2012)
- Hyndman, R.J., Ullah, M.S.: Robust forecasting of mortality and fertility rates: A functional data approach. *Computational Statistics & Data Analysis* **51**(10), 4942–4956 (2007)
- Karhunen, K.: Zur spektraltheorie stochastischer prozesse. *Ann. Acad. Sci. Fennicae, AI* **34** (1946)
- Kokoszka, P., Miao, H., Zhang, X.: Functional dynamic factor model for intraday price curves. *Journal of Financial Econometrics* **13**(2), 456–477 (2015)
- Liebl, D.: Modeling and forecasting electricity spot prices: A functional data perspective. *The Annals of Applied Statistics*, 1562–1592 (2013)
- Lam, C., Yao, Q., Bathia, N.: Estimation of latent factors for high-dimensional time series. *Biometrika* **98**(4), 901–918 (2011)
- Martínez-Hernández, I., Genton, M.G.: Surface time series models for large spatio-temporal datasets. *Spatial Statistics* **53**, 100718 (2023)
- Martínez-Hernández, I., Gonzalo, J., González-Farías, G.: Nonparametric estimation of functional dynamic factor model. *Journal of Nonparametric Statistics* **34**(4), 895–916 (2022)
- Nie, Y., Wang, L., Liu, B., Cao, J.: Supervised functional principal component analysis. *Statistics and Computing* **28**(3), 713–723 (2018)

- Peña, D., Poncela, P.: Nonstationary dynamic factor analysis. *Journal of Statistical Planning and Inference* **136**(4), 1237–1257 (2006)
- Panaretos, V.M., Tavakoli, S.: Fourier analysis of stationary time series in function space. *The Annals of Statistics*, 568–603 (2013)
- Peña, D., Yohai, V.J.: Generalized dynamic principal components. *Journal of the American Statistical Association* **111**(515), 1121–1131 (2016)
- Ramsay, J.O., Silverman, B.W.: *Functional data analysis*, 2nd edn. Springer (2005)
- Shang, H.L.: A survey of functional principal component analysis. *AStA Advances in Statistical Analysis* **98**, 121–142 (2014)
- Shang, H.L., Kearney, F.: Dynamic functional time-series forecasts of foreign exchange implied volatility surfaces. *International Journal of Forecasting* **38**(3), 1025–1049 (2022)
- Smucler, E.: Consistency of generalized dynamic principal components in dynamic factor models. *Statistics & Probability Letters* **154**, 108536 (2019)
- Stock, J.H., Watson, M.W.: Testing for common trends. *Journal of the American statistical Association* **83**(404), 1097–1107 (1988)
- Stock, J.H., Watson, M.W.: Forecasting using principal components from a large number of predictors. *Journal of the American statistical association* **97**(460), 1167–1179 (2002)
- Viviani, R., Grön, G., Spitzer, M.: Functional principal component analysis of fmri data. *Human Brain Mapping* **24**(2), 109–129 (2005)
- Yang, Y., Shang, H.L., Raymer, J.: Forecasting australian fertility by age, region, and birthplace. *International Journal of Forecasting* (2022)